



A generalized theoretical approach for solar cells fill factors by using Shockley diode model and Lambert W-function: A review comparing theory and experimental data

Simón Roa Díaz

Instituto Balseiro - UNCuyo, CONICET- INN - CNEA, Av. E. Bustillo 9500, R8402AGP, San Carlos de Bariloche, Río Negro, Argentina

ARTICLE INFO

Keywords:
 Solar cells
 Fill factor
 Shockley diode model
 Lambert W-Function

ABSTRACT

Solar Cells (SCs) energy-conversion technologies have been widely studied from their physical fundamentals to potential commercial applications. In particular, SCs Fill Factors (FFs) are a key factor for evaluating the transport efficiency of the photo-generated current and consequently the potential photovoltaic of the device. However, FF dependence on other solar cell relevant electronic properties is not entirely clear, blurring the physical meaning of this factor. In this context, this work reports the derivation of a self-consistent and generalized analytical equation by using simple Shockley diode equation and Lambert W-function that explicitly relates solar cells FFs with simple key electronic parameters. The photo-generated (J_L)-to-reverse saturation (J_0) current density ratio (J_L/J_0) was the key parameter considered for this approach because of its considerable limiting impact on FF magnitude. The accuracy of this equation was tested by an exhaustive contrast with a wide variety of experimental data for different solar cells technologies.

1. Introduction

Nowadays, solar cells-based energy conversion technologies have been widely studied from the theoretical fundamentals to their potential industrial aspects because of the increasing demand for new renewable energy alternatives [1–5]. For applications at great scale, solar cells Power Conversion Efficiencies (PCEs) and Fill Factors (FFs) are critical parameters to evaluate their photovoltaic performance and possible commercial distribution.

To practical effects, solar cells with the highest possible PCEs and FFs values are desired, but also looking for an optimum compromise with fabrication costs. Typically, different high-PCE and high-FF solar cells technologies are commonly based on Silicon (Si) [6,7], Copper Indium Gallium Selenide (CIGS) [8–10], Copper Zinc Tin Sulfide (CZTS) [11, 12], Perovskites (PCS) [13–15], organic or synthetic dyes (DSSC) [16–18], III-V semiconductors (GaAs and InP, for example) [19–22], II-VI semiconductors (CdTe, CdS and ZnO, for example) [23–27] and IV-VI semiconductors (mainly PbS, PbSe and PbTe) [27–30]. In general, these kind of solar cells can be electronically well-represented by using a simple diode equivalent circuit model (see Fig. 1).

From Fig. 1, the photo-generated current (I_L) can be calculated as:

$$I_L = I_D + I' \quad (1)$$

where $I_D := I_D(V)$ and I' represent the diode characteristic current-voltage ($I - V$) behavior and an auxiliary current, respectively. Moreover, the following equation can be deduced:

$$I' = I_{sh} + I, \quad (2)$$

where I_{sh} and I are the shunt current and the effective current flowing through the solar cell, respectively. So, the solar cell characteristic $I - V$ behavior can be described combining Eqs. (1) and (2) as:

$$I = I_L - I_D - I_{sh}. \quad (3)$$

Considering a diode current I_D well-described by the Shockley diode equation [31], Eq. (3) can be re-write as follows:

$$I = I_L - I_0 \left[e^{\frac{V+IR_s}{nV_T}} - 1 \right] - \frac{V + IR_s}{R_{sh}}, \quad (4)$$

where I_0 is the reverse saturation current, n the diode quality factor (1 for ideal diode), and $V_T = kT/q$ the thermal voltage. At room temperature ($T = 300$ K), $V_T \approx 25.9$ [mV]. Here, the equivalence $I_{sh} = (V + IR_s)/R_{sh}$ can be easily deduced by analyzing the equivalent circuit shown in Fig. 1. It is more common to use Eq. (4) in terms of the current density (J , in [mA/cm^2]) instead simple current. Thus, this

E-mail address: sroadaz8@gmail.com.

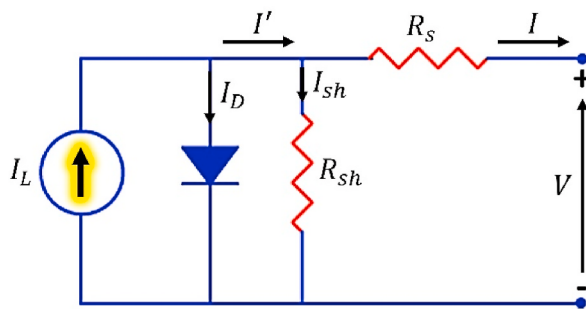


Fig. 1. Equivalent circuit of a solar cell considering the single diode model. In this case, parasitic series (R_s) and shunt (R_{sh}) resistances are also considered.

equation can be re-write (normalizing by cell active area (A_c)) as follows [1,2]:

$$J = J_L - J_0 \left[e^{\frac{V+JR_s}{nV_T}} - 1 \right] - \frac{V + JR_s}{R_{sh}}. \quad (5)$$

Most of high-PCE and high-FF solar cells (based on the materials previously mentioned) usually present n and J_0 values in ranges of 1–2 and $10^{-10} - 10^{-5}$ [mA/cm²] [6–30,32–45], respectively. These kinds of cells generally exhibit very high photo-generated current densities (10–50 [mA/cm²]) concerning the reverse saturation ones ($J_L / J_0 \gg 1$), which is a characteristic feature of High Quality Solar Cells (HQSCs). In general, it is also observed that HQSCs present very high shunt resistances ($R_{sh} \sim 10^3 - 10^6$ [$\Omega \cdot \text{cm}^2$]) concerning the parasitic series ones ($R_s \sim 10^{-1} - 10^0$ [$\Omega \cdot \text{cm}^2$]) [32–45], usually implying $J \cong J_L - J_0$ since $J_L - J_0 \gg V + JR_s / R_{sh}$ for voltages (V) and current densities (J) in ranges of 0–1 [V] and 0–50 [mA/cm²]. Under this approximation (well-known as the $R_s \neq 0 - R_{sh} \rightarrow \infty$ condition), Eq. (5) can be simplified as:

$$J = J_L - J_0 \left[e^{\frac{V}{nV_T}} - 1 \right]. \quad (6)$$

This model is generally well-accepted for HQSCs (high-PCE and high-FF solar cells). A generalized representation of this equation for a high-FF solar cell ($FF \sim 88\%$) is shown in Fig. 2. In this case, the $J - V$ behavior is modeled as a simple effective diode in dark-condition ($J_L = 0$) and the photovoltaic response as a simple current-shifting by the influence of the photo-generated current density (J_L). Here it is defined the short-circuit current density ($J_{sc} = J(V=0) \cong J_L$) and the open-circuit voltage (V_{oc} , being $J(V=V_{oc}) = 0$). For HQSCs, the condition $J_L \cong J_{sc}$ is commonly

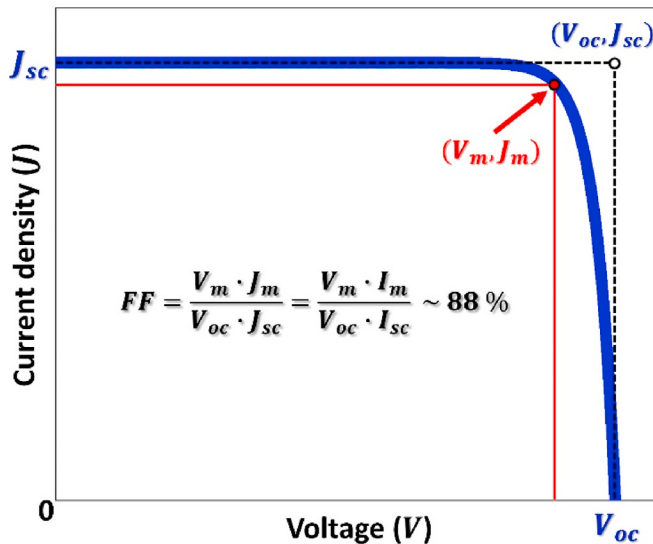


Fig. 2. Scheme of the typical $J - V$ behavior observed for a HQSCs.

satisfied for $J_{sc} \gg J_0$, which is typically observed in practice [6–30, 32–45].

J_{sc} and V_{oc} represent the potential maximum current density and voltage from a solar cell, respectively. However, intrinsic defects (like lattice mismatch, dislocations, grain boundaries, polycrystallinity, topological defects, etc.) coming from the semiconducting homo/hetero junctions, that make up the solar cell active area, limit the possibility of achieving this maximum potential. This current density and voltage drop from the maximum potential is represented by the “real” maximum values J_m and V_m , which are associated with the solar cell maximum power ($P_m = I_m V_m = J_m A_c V_m$).

To quantify the mentioned effect, the parameter FF is introduced and commonly described as follows [1,2]:

$$FF = \frac{V_m \cdot J_m}{V_{oc} \cdot J_{sc}} = \frac{V_m \cdot J_m}{V_{oc} \cdot J_{sc}}, \quad (7)$$

representing how close is the solar cell to reach its maximum potential photovoltaic performance. Graphically, V_m is a measure of the “squareness” of the solar cell and is also the area of the largest rectangle (“real” maximum performance for J_m for $J - V$) which will fit in the curve, as shown in Fig. 2. So, $J - V$ curves tending to be more “squared” will be typical of solar cells with higher FF s. The particular example shown in Fig. 2 corresponds to a high-FF solar cell based on silicon technologies, which usually enable to fabricate cells with $FF > 70\%$ [32–45].

While FF has a well-defined analytical equation as described by Eq. (7), its multivariable nature does not enable an intuitive understanding about the fundamental physics behind it. Moreover, solar cells FF s dependence on other simple and relevant electronic properties is not entirely clear, clearing the physical meaning of this factor.

In this context, this work reports the derivation of a self-consistent and generalized analytical equation by using Lambert W-function that explicitly relates solar cells FF s with a simple key electronic parameter. The J_L/J_0 ratio was the key parameter considered for this approach because of its critical limiting impact on FF magnitude. The accuracy of this equation was tested by an exhaustive contrast with a wide variety of experimental data for different solar cells technologies based on materials like those previously mentioned.

2. Theoretical analysis

Considering that the $J - V$ behavior of HQSCs can be well-described by Eq. (6), this can be simplified at the open-circuit voltage (V_{oc}) condition as:

$$0 = J_L - J_0 \left[e^{\frac{V_{oc}}{nV_T}} - 1 \right], \quad (8)$$

which allows to calculate V_{oc} as follows:

$$V_{oc} = nV_T \ln \left(\frac{J_L}{J_0} + 1 \right) \text{ or } V_{oc} = nV_T \ln \left(\frac{I_L}{I_0} + 1 \right). \quad (9)$$

On the other hand, the maximum voltage (V_m) can be estimated finding the point of maximum power (P_m), which can be calculated by a first-order derivation of the power (P)-voltage (V) curve by the following way:

$$P = I \cdot V = JA_c \cdot V = I_L V - I_0 V \left[e^{\frac{V}{nV_T}} - 1 \right] \quad (10)$$

$$\rightarrow \frac{dP}{dV} = I_L + I_0 - I_0 \frac{d}{dV} \left(V e^{\frac{V}{nV_T}} \right) = \dots = I_L + I_0 - I_0 e^{\frac{V}{nV_T}} \left[\frac{V}{nV_T} + 1 \right]. \quad (11)$$

Consequently, at the point of maximum power the following condition is satisfied:

$$\frac{dP}{dV} = 0 = I_L + I_0 - I_0 e^{\frac{V_m}{nV_T}} \left[\frac{V_m}{nV_T} + 1 \right] \quad (12)$$

$$\rightarrow \frac{I_L + I_0}{I_0} = \frac{I_L}{I_0} + 1 = \frac{J_L}{J_0} + 1 = e^{\frac{V_m}{nV_T}} \left[\frac{V_m}{nV_T} + 1 \right]. \quad (13)$$

Considering that HQSCs generally present $J_{sc} \cong J_L \gg J_0$ (or $J_L/J_0 \gg 1$, as discussed in section 1) and V_m values varying from 0.5 to 1 [V] [32–45] such that $V_m/nV_T \gg 1$ (for $n = 1\text{--}2$ and $T = 300$ K), Eq. (13) can be considerably simplified as follows:

$$\frac{J_L}{J_0} = \frac{V_m}{nV_T} e^{\frac{V_m}{nV_T}}. \quad (14)$$

Analyzing Eq. (14), it can be observed that the solution of this equation for V_m is not trivial. In fact, there is no way to find analytically a solution for this equation by conventional calculus-based methods. Conveniently, a solution for equations with this functional form was already reported long time ago [46,47]. This solution can be found by using Lambert W -function [46], which is a multivalued function that contains the branches of the inverse relation of the $f(w) = we^w$ function, where w is any complex number.

Lambert stated that for each integer k there is one branch ($W_k(z)$) that is a complex-valued function of one complex argument, being W_0 the **principal branch**. These functions have the following property if z and w are any complex number:

$$we^w = z, \quad (15)$$

and holds if and only if:

$$w = W_k(z), \text{ for some integer } k. \quad (16)$$

When dealing only with real numbers, the two branches W_0 and W_{-1} suffice the equation (for real numbers x and y):

$$ye^y = x, \quad (17)$$

and can be solved for y only if $x \geq -1/e$. In this case, we get $y = W_0(x)$ if $x \geq 0$ and the two $y = W_0(x)$ and $y = W_{-1}(x)$ if $-1/e \leq x < 0$. In

$$\begin{aligned} W_0(x) &= \sum_{n=1}^{\infty} \frac{(-n)^{n-1}}{n!} x^n = \dots \\ &\dots = x - x^2 + \frac{3}{2}x^3 - \frac{8}{3}x^4 + \frac{125}{24}x^5 - \dots, \end{aligned} \quad (18)$$

being $1/e$ the convergence radius, as may be seen by the Cauchy ratio test [49]. The function defined by this series can be extended to a holomorphic function defined on all complex numbers with a branch cut along the interval $(-\infty, -1/e]$; this holomorphic function defines the principal branch of the Lambert W -function. For large values of x , $W_0(x)$ is asymptotic to:

$$\begin{aligned} W_0(x) &= L_1 - L_2 + \frac{L_2}{L_1} + \dots \\ &\dots + \frac{L_2(-2+L_2)}{2L_1^2} + \frac{L_2(6-9L_2+2L_2^2)}{6L_1^3} + \dots \\ &\dots + \frac{L_2(-12+36L_2-22L_2^2+3L_2^3)}{12L_1^4} + \dots = \dots \\ &\dots = L_1 - L_2 + \sum_{l=0}^{\infty} \sum_{m=1}^{\infty} \frac{(-1)^l}{m!} \begin{bmatrix} l+m \\ l+1 \end{bmatrix} L_1^{-l-m} L_2^m = \dots \\ &\dots = L_1 - L_2 + S_{l,m}(L_1, L_2) \end{aligned} \quad (19)$$

where $L_1 = \ln(x)$, $L_2 = \ln[\ln(x)]$, and $\begin{bmatrix} l+m \\ l+1 \end{bmatrix}$ is a non-negative Stirling number of the first kind [46]. Thus, V_m can be estimated as:

$$V_m = nV_T W_0 \left(\frac{J_L}{J_0} \right) = nV_T \left[\ln \left(\frac{J_L}{J_0} \right) - \ln \left[\ln \left(\frac{J_L}{J_0} \right) \right] + \dots \right]. \quad (20)$$

Using Eq. (20) and Eq. (9), Eq. (7) for FF can be re-defined as:

$$\begin{aligned} FF &= \frac{V_m \cdot J_m}{V_{oc} \cdot J_{sc}} = \left(\frac{J_m}{J_L} \right) \frac{nV_T W_0(J_L/J_0)}{nV_T \ln(J_L/J_0)}, \quad \frac{J_L}{J_0} \gg 1 \text{ and } J_L \cong J_0 \\ FF &= \frac{W_0(J_L/J_0)}{\ln(J_L/J_0)} \frac{J_m}{J_L} = \frac{W_0(J_L/J_0)}{\ln(J_L/J_0)} \left(\frac{J_L - J_0 e^{\frac{V_m}{nV_T}}}{J_L} \right); e^{\frac{V_m}{nV_T}} \gg 1 \\ FF &= \frac{W_0(J_L/J_0)}{\ln(J_L/J_0)} \frac{J_m}{J_L} = \frac{W_0(J_L/J_0)}{\ln(J_L/J_0)} \left(1 - \frac{J_0}{J_L} e^{W_0(J_L/J_0)} \right) = \dots \\ \dots &= 1 - \left(\frac{\ln[\ln(J_L/J_0)]}{\ln(J_L/J_0)} \right) + \frac{S_{l,m}(L_1, L_2)}{\ln(J_L/J_0)} - \dots \\ \dots &- \frac{W_0(J_L/J_0)}{\ln(J_L/J_0)} \frac{J_0}{J_L} e^{W_0(J_L/J_0)}. \end{aligned} \quad (21)$$

particular, the Lambert W relation cannot be expressed in terms of elementary functions [48].

Comparing with Eq. (14), we can observe the similarity between the Lambert W -function problem and that associated with determining V_m . By simple inspection, the problem can be set for $x = J_L/J_0$ and $y = V_m/nV_T$. In this case, x is clearly ≥ 0 since it is assumed that $J_L \gg J_0$. Thus, the problem is reduced to find the $W_0(x)$ function.

The Taylor series of $W_0(x)$ around $x = 0$ can be found using the Lagrange inversion theorem [47] as follows:

Here, we simplify Eq. (21) as:

$$FF = 1 - \phi(J_L/J_0), \quad (22)$$

where the function $\phi(J_L/J_0)$ implicitly contains all the effects associated with current dissipation mechanisms that limit the solar cell fill factor and move away it from the ideal behavior $FF = 1$.

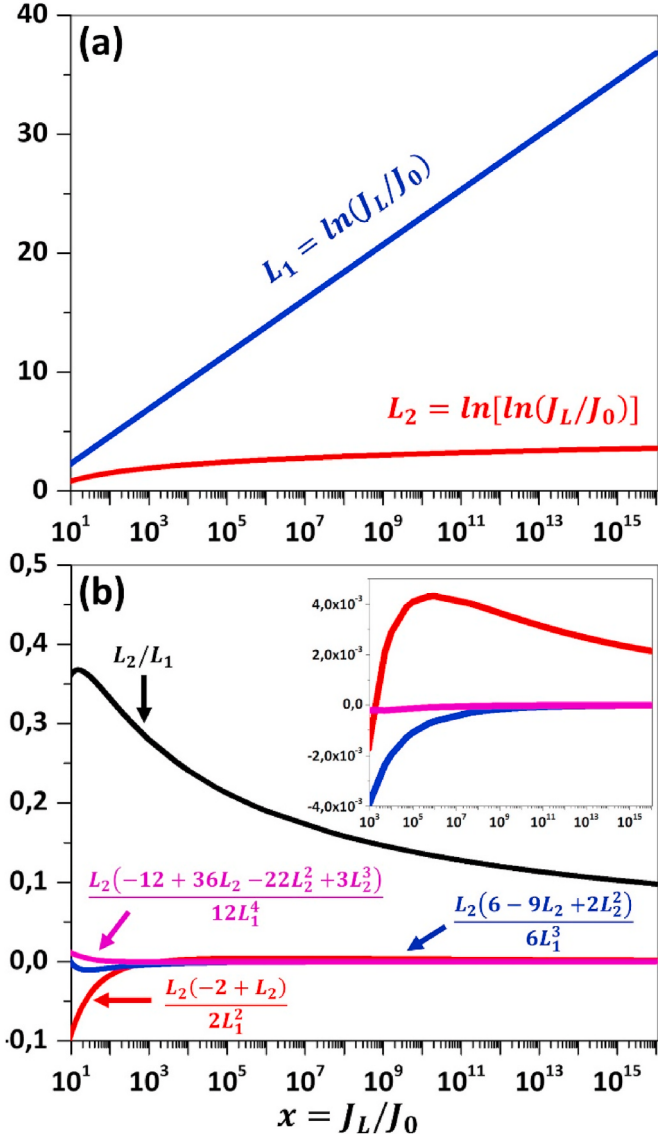


Fig. 3. (a) Evolution of the functions L_1 and L_2 with respect to the J_L / J_0 ratio. The (b) evolution of the first four terms of the series $S_{l,m}(L_1, L_2)$ with respect to the J_L / J_0 ratio is also shown.

3. Results and discussion

3.1. Analyzing the properties of the $W_0(x)$ function

In certain x regimes, the $W_0(x)$ function present very interesting properties that can be used for reducing the problem and achieving a simple analytical expression for FF concerning Eq. (21). Considering the fundamental terms that define this function (L_1 and L_2 in Fig. 3(a)), we can observe that the terms of the series $S_{l,m}(L_1, L_2)$ present different orders of relevance as shown in Fig. 3(b). In this figure, the values of the first four terms of the series for $x = J_L / J_0 \geq 10$ are shown.

Considering that HQSCs can present J_L / J_0 ratios in the order of 10^4 for very pessimistic cases [32–45], being commonly $J_L / J_0 > 10^6$, we can see from inset graph in Fig. 3(b) that the first term $L_2 / L_1 (\sim 10^{-1})$ of the series $S_{l,m}(L_1, L_2)$ clearly dominates over the others ($< 5 \times 10^{-3}$) such that their contributions could be easily neglected. Thus, only considering the first term of this series, the function $W_0(J_L / J_0)$ can be defined as follows:

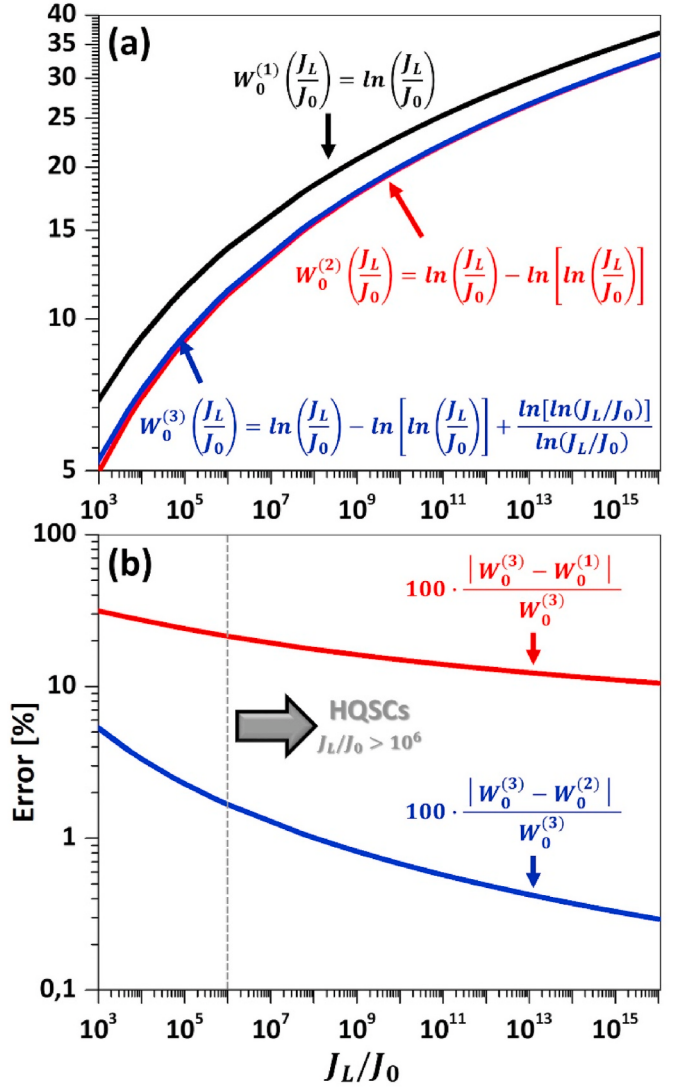


Fig. 4. (a) Evolution of the function $W_0(J_L / J_0)$ (Eq. (23)) considering the first one ($W_0^{(1)}$), the first two ($W_0^{(2)}$) and the three terms ($W_0^{(3)} := W_0(J_L / J_0)$) of this function. The (b) evolution of the errors associated with these approaches are also shown.

$$W_0\left(\frac{J_L}{J_0}\right) \cong \ln\left(\frac{J_L}{J_0}\right) - \ln\left[\ln\left(\frac{J_L}{J_0}\right)\right] + \frac{\ln[\ln(J_L / J_0)]}{\ln(J_L / J_0)}. \quad (23)$$

Eq. (23) can be still reduced by a simple analysis of the weight of each term, as shown in Fig. 4(a). Note that only considering the first term $\ln(J_L / J_0) = W_0^{(1)}$ the real behavior of the W_0 function ($:= W_0^{(3)}$ in Fig. 4(a)) is not well represented, especially for the regime of low J_L / J_0 ratios. Nevertheless, this behavior can be well represented by considering the first two terms ($W_0^{(2)}$), as shown in Fig. 4(a). The approach given by function $W_0^{(2)}$ is reasonable considering the typical ranges for the J_L / J_0 ratios observed in HQSCs ($> 10^6$), which enabled to estimate the value of the function $W_0(J_L / J_0)$ with an error lower than 2% (see Fig. 4(b)).

Thus, considering the low error associated with the approach given by the function $W_0^{(2)}$, we can provide the following simple analytical expression for calculating V_m :

$$V_m \cong n V_T \left(\ln\left(\frac{J_L}{J_0}\right) - \ln\left[\ln\left(\frac{J_L}{J_0}\right)\right] \right). \quad (24)$$

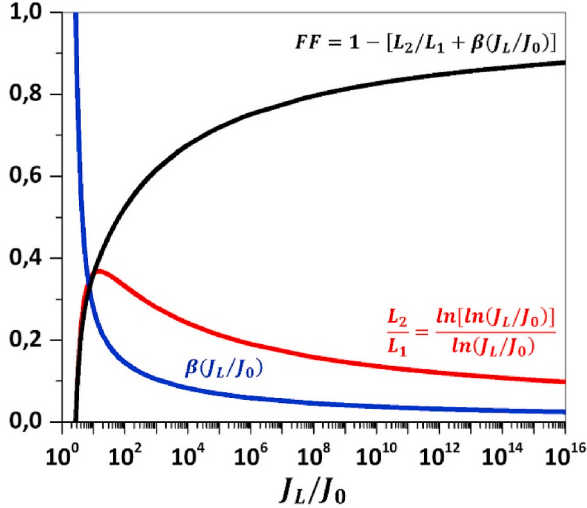


Fig. 5. Evolution of the functions $\beta(J_L/J_0)$, L_2/L_1 and FF (Eq. (25)) with respect to the J_L/J_0 ratio.

3.2. Proposing an exact analytical equation for FF by using $W_0(x)$ function

Using Eq. (24), a generalized equation for the solar cells fill factors in terms of J_L/J_0 is given as:

$$\begin{aligned} FF &= \frac{W_0(J_L/J_0)}{\ln(J_L/J_0)} \left(1 - \frac{J_0}{J_L} e^{W_0(J_L/J_0)} \right) = \dots \\ \dots &= \left(1 - \frac{\ln[\ln(J_L/J_0)]}{\ln(J_L/J_0)} \right) \left(1 - \frac{J_0}{J_L} e^{W_0(J_L/J_0)} \right) = \dots \\ \dots &= 1 - \frac{\ln[\ln(J_L/J_0)]}{\ln(J_L/J_0)} - \dots \\ \dots &- \frac{J_0}{J_L} e^{W_0(J_L/J_0)} \left(1 - \frac{\ln[\ln(J_L/J_0)]}{\ln(J_L/J_0)} \right) = \dots \\ \dots &= 1 - [L_2/L_1 + \beta(J_L/J_0)], \end{aligned} \quad (25)$$

where it is defined:

$$\beta(J_L/J_0) = \frac{J_0}{J_L} e^{W_0(J_L/J_0)} \left(1 - \frac{\ln[\ln(J_L/J_0)]}{\ln(J_L/J_0)} \right). \quad (26)$$

Fig. 5 shows the different influence magnitude order of both functions (L_2/L_1 and $\beta(J_L/J_0)$) on the FF magnitude. From this graph, we can see that generally the value of the L_2/L_1 function is considerably higher than the $\beta(J_L/J_0)$ one for $J_L/J_0 > 10^1$. However, in the most pessimistic of cases, $\beta(J_L/J_0)$ is about of a 25% of the value of L_2/L_1 (for $J_L/J_0 = 10^{16}$). So, this term should be not neglected to practical effects.

An interesting behavior can be observed for the $J_L/J_0 < 10^1$ regime, where the contribution of the $\beta(J_L/J_0)$ becomes critically important and that associated with the L_2/L_1 one decays abruptly. To practical effects, at the neighborhood of this regime, the fill factor shows an accelerated and critical drop. These results clearly evidence the critical influence of the J_L/J_0 ratio on the solar cells fill factors, showing the key role of this ratio on limiting the potential photovoltaic performance of solar cells.

Poor-quality solar cells are characterized by low fill factors (not necessarily implying low PCEs) which are usually associated with high diode quality factors (n) [32–45]. High diode quality factors mean that recombination currents are flowing not homogeneously in the solar cell because of high defect concentration zones at local sites [50]. Important defects in the diode-like junction structures of solar cells can be introduced by interfacial roughness as well as lattice structure mismatch [51]. In solar cells based on hetero-junctions, which typically involve

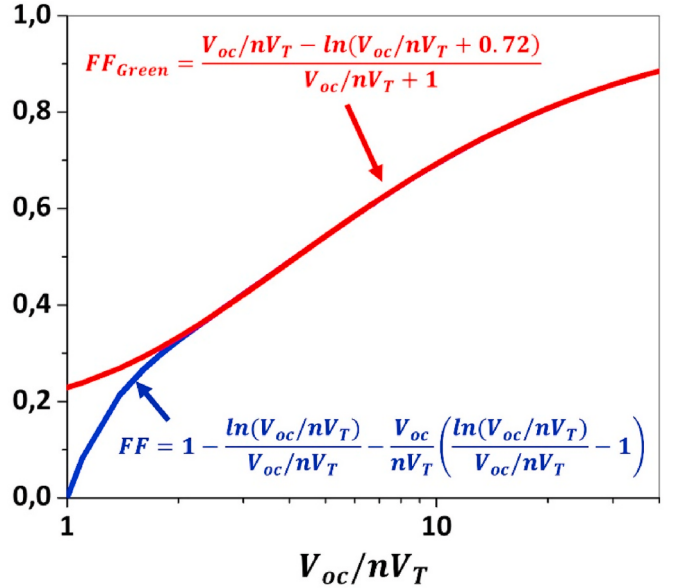


Fig. 6. Comparison between the empirical approach given by Green (Eq. (28)) and that theoretical proposed in this work. (Eq. (27)). (For interpretation of the references to colour in this figure legend, the reader is referred to the Web version of this article.)

lattice structure mismatch, these effects can be intensified and affect negatively the electron transport efficiency and recombination at the interfaces neighborhood. For this reason, this kind of solar cells usually present considerably lower FF concerning cells based on homojunctions like the silicon ones ($FF > 75\%$) [32–45].

Regarding the previous point, it is important to mention that there is a correlation between n and J_L/J_0 . Physically, it is reasonable that the fill factor decreases as the J_L/J_0 decreases since, considering that J_L keeps in the order of 10^1 [mA/cm^2], high J_0 currents involves considerable dissipation of photo-generated current because it favors the recombination of the charge carriers at the interfaces of the solar cells active layers [50]. Thus, high J_0 currents typically involves high n values, i.e., poor quality diode-like junctions in solar cells that considerable limit FF .

The correlation between n and J_L/J_0 can be easily seen by considering the definition of $V_{oc} = nV_T \ln(J_L/J_0)$ (for $J_L/J_0 \gg 1$) and replacing in Eq. (25) as follows:

$$FF = 1 - \frac{\ln(V_{oc}/nV_T)}{V_{oc}/nV_T} - \frac{V_{oc}}{nV_T} \left(\frac{\ln(V_{oc}/nV_T)}{V_{oc}/nV_T} - 1 \right), \quad (27)$$

A similar and widely extended expression, but empirically determined, was proposed by Green [52,53]:

$$FF_{Green} = \frac{v_{oc} - \ln(v_{oc} + 0.72)}{v_{oc} + 1}, \quad (28)$$

where $v_{oc} = V_{oc}/nV_T$. From Fig. 6 it can be observed the similarity between the empirical Green's equation and the theoretical one derived in this work. In particular, both functions match almost perfectly (with errors lower than 0.2% concerning the empirical reference) for $V_{oc}/nV_T \geq e$ or equivalently for $J_L/J_0 \geq e^e \sim 15.15$.

Note that both empirical and theoretical approaches considerably differ one from each other at the regime of very low $V_{oc}/nV_T (< e)$ or equivalently low $J_L/J_0 (< e^e \sim 15.15)$. This difference is expected because the theoretically proposed equation is based on the hypothesis of $R_s \neq 0$ and $R_{sh} \rightarrow \infty$, which is not valid for solar cells with very low J_L/J_0 ratios or very low FF s. However, considering that typically $J_L/J_0 > 10^6$ for HQSCs [32–45], we can assume the presented theoretical approach is more than satisfactory to represent the generalized fill factor behavior for solar cells. This approach also corresponds to a theoretical



Fig. 7. Different photo-generated $J - V$ curves reported by Green et al [32–38] for solar cells based on different kinds of technologies. Solar cells based on materials like Si, CIGS, CZTS, Perovskites, DSSC, III-V and II-VI semiconductors are shown. Red solid curves correspond to Eq. (6) fit. (For interpretation of the references to colour in this figure legend, the reader is referred to the Web version of this article.)

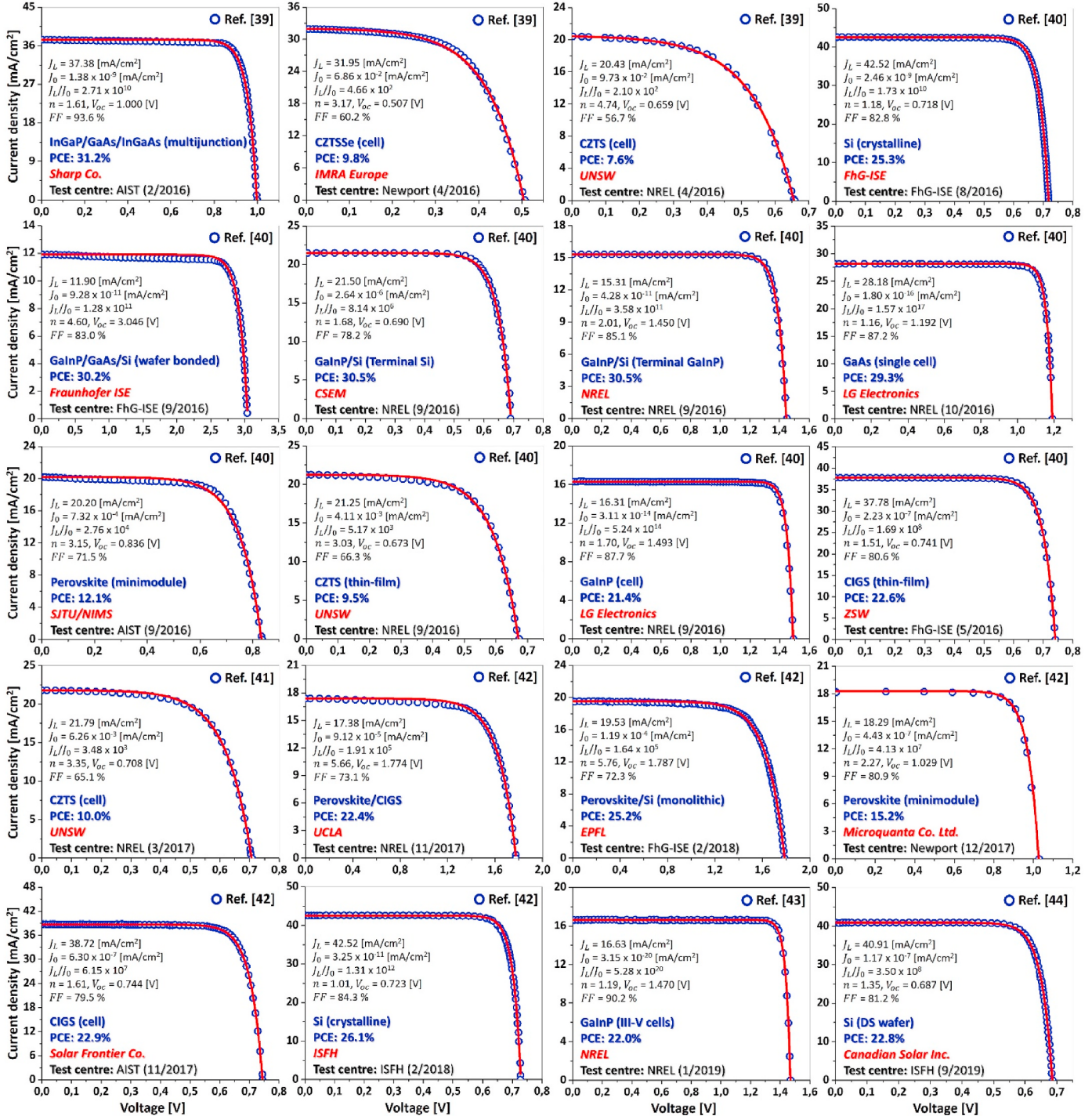


Fig. 8. Different photo-generated $J - V$ curves reported by Green et al [39–44] for solar cells based on different kinds of technologies. Solar cells based on materials like Si, CIGS, CZTS, Perovskites and III-V semiconductors are shown. Red solid curves correspond to Eq. (6) fit. (For interpretation of the references to colour in this figure legend, the reader is referred to the Web version of this article.)

verification of the well-known empirical Green's equation for solar cells fill factors.

3.3. Experimental validation of the theoretically-estimated equation for FF

The theoretical approach proposed in this work was validated by contrasting with considerable experimental data. Different photo-generated $J - V$ curves reported by Green et al [32–44] (see Figs. 7 and 8) for solar cells based on different kinds of technologies were used

for this purpose. Solar cells based on materials like Silicon (Si), Copper Indium Gallium Selenide (CIGS), Copper Zinc Tin Sulfide (CZTS), Perovskites (PCS), organic or synthetic dyes (DSSC), III-V (GaAs and InP) and II-VI (CdTe) semiconductors were considered. In Figs. 7 and 8 are also indicated some relevant parameters of each solar cell such as J_L , J_0 , J_L/J_0 , n , V_{oc} and experimentally determined FF . All of these parameters, expect FF , were estimated by using the photo-generated Shockley diode equation (Eq. (6)). These fits correspond to the red solid lines shown in both figures.

In general, Eq. (6) model presented a very good agreement with

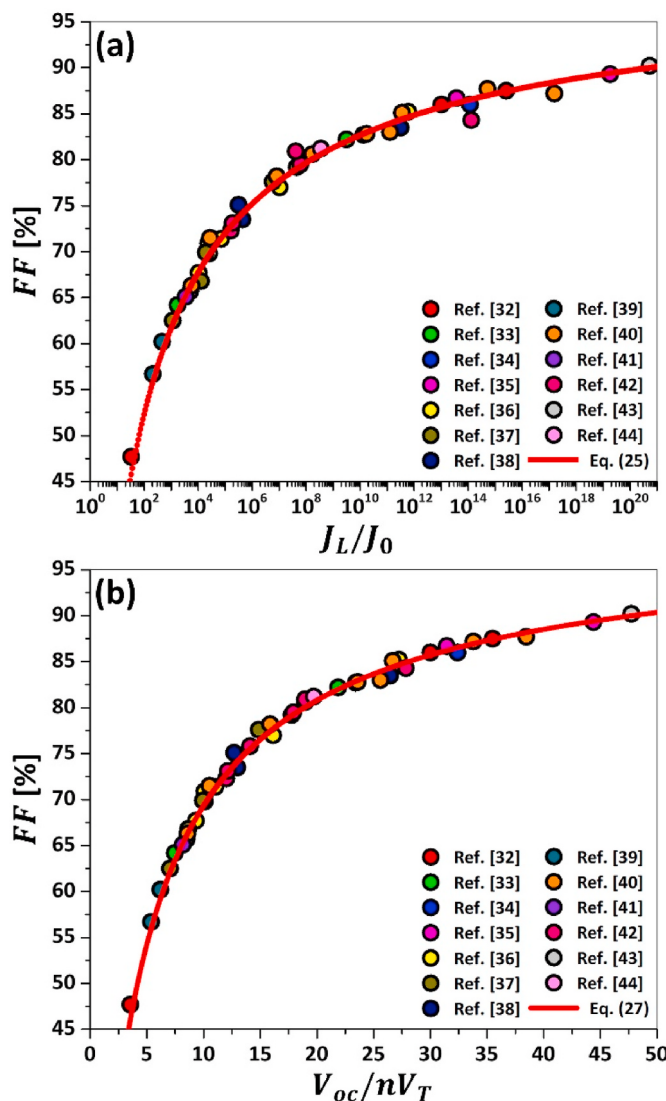


Fig. 9. Comparison between the experimental and theoretical approaches for FF in different kinds of solar cells with respect to the (a) J_L/J_0 and (b) V_{oc}/nV_T ratios. The red solid lines and circular filled symbols correspond to theoretical approaches and experimental data, respectively. (For interpretation of the references to colour in this figure legend, the reader is referred to the Web version of this article.)

experimental $J - V$ curves, observing determination coefficients (R^2) higher than 0.98. From this equation, n and J_L/J_0 values in the ranges of 1.01–7.80 and 3.31×10^1 – 5.28×10^{20} were estimated, respectively. Solar cells based on Si and III-V semiconductors usually presented the highest J_L/J_0 ratios ($>10^9$). On the other hand, solar cells based on other technologies usually presented the lowest J_L/J_0 ratios ($<10^7$).

Fig. 9 shows a comparison between the experimental [32–44] and theoretical approaches (Eqs. (25) and (27)) for FF in different kinds of solar cells with respect to the J_L/J_0 and V_{oc}/nV_T ratios. From Fig. 9(a) and (b), we can observe the very good agreement between the experimental tendency and the theoretical approaches proposed in this work (Eqs. (25) and (27)). In general, the theoretical approaches enable to estimate FF values with uncertainties lower than 3% concerning the experimental data. This result validates the hypotheses set for the theoretical formulation of Eqs. (25) and (27), particularly showing the good accuracy of the Shockley diode model for describing the photo-generated $J - V$ response of solar cells. The good agreement observed in Fig. 9(a) and (b) is self-consistent with this fact.

As previously discussed, theoretical and now experimental data

show the critical impact of the J_L/J_0 ratio (directly associated with the quality of diode junctions which make up the solar cell) on the solar cells potential performance. It can be seen that FF begins to dramatically drop for the regime $J_L/J_0 < 10^6$, which is typical of new generation solar cells like those based on organic components (DSSC), Perovskites or CZTS. This fact indicates that solar cells performance is strongly limited by the interfaces quality (where defects are introduced by combining materials with very heterogeneous physical properties), which directly impacts on the J_L/J_0 magnitude and take away solar cells from the ideal diode behavior (maximization of FF).

4. Conclusions

A generalized theoretical approach to estimate the solar cells fill factors, in terms of relevant photovoltaic parameters like J_L/J_0 and V_{oc}/nV_T , by using the simple Shockley diode model and Lambert W-function was successfully achieved. A very good agreement between the theoretical approach proposed in this work and several experimental data for solar cells based on different kinds of technologies was observed. Theoretical approaches enabled to estimate FFs values with uncertainties lower than 3% concerning the experimental data, validating the accuracy of Shockley model and Lambert W-function for modeling the photo-generated $J - V$ response of a wide variety of solar cells. Equations derived in this work allowed to understand the effective magnitude order of the influence of relevant physical parameters like J_L/J_0 on the solar cells potential photovoltaic performance, particularly helping to uncover the physical meaning of the solar cells fill factors.

Credit author statement

Simón Roa: Conceptualization, Methodology, Validation, Formal analysis, Investigation, Writing - Original Draft, Writing - Review & Editing, Visualization, Project administration.

Declaration of competing interest

The authors declare that they have no known competing financial interests or personal relationships that could have appeared to influence the work reported in this paper.

References

- [1] S. Sharma, K.K. Jain, A. Sharma, Solar cells: in research and applications—A review, Mater. Sci. Appl. 6 (2015) 1–11, <https://doi.org/10.4236/msa.2015.612113>.
- [2] P.K. Nayak, S. Mahesh, H.J. Snaith, D. Cahen, Photovoltaic solar cell technologies: analyzing the state of the art, Nature Reviews Materials 4 (2019) 269–285, <https://doi.org/10.1038/s41578-019-0097-0>.
- [3] D.G. Moon, S. Rehan, D.H. Yeon, S.M. Lee, S.J. Park, S. Ahn, Y.S. Cho, A review on binary metal sulfide heterojunction solar cells, Sol. Energy Mater. Sol. Cell. 200 (2019) 109963, <https://doi.org/10.1016/j.solmat.2019.109963>.
- [4] P. Roy, N.K. Sinha, S. Tiwari, A. Khare, A review on perovskite solar cells: evolution of architecture, fabrication techniques, commercialization issues and status, Sol. Energy 198 (2020) 665–688, <https://doi.org/10.1016/j.solener.2020.01.080>.
- [5] M.R.N. Thomas, V.J.K. LourduSamy, A.A. Dhandayuthapani, V. Jayakumar, Non-metallic organic dyes as photosensitizers for dye-sensitized solar cells: a review, Environ. Sci. Pollut. Control Ser. (2021), <https://doi.org/10.1007/s11356-021-13751-7>.
- [6] Y. Lee, C. Park, N. Balaji, Y.-J. Lee, V.A. Dao, High-efficiency silicon solar cells: a review, Isr. J. Chem. 55 (2015) 1050–1063, <https://doi.org/10.1002/ijch.201400210>.
- [7] Y. Xing, P. Han, S. Wang, P. Liang, S. Lou, Y. Zhang, S. Hu, H. Zhu, C. Zhao, Y. Mi, A review of concentrator silicon solar cells, Renew. Sustain. Energy Rev. 51 (2015) 1697–1708, <https://doi.org/10.1016/j.rser.2015.07.035>.
- [8] J. Ramanujam, U.P. Singh, Copper indium gallium selenide based solar cells – a review, Energy Environ. Sci. 10 (2017) 1306–1319, <https://doi.org/10.1039/C7EE00826K>.
- [9] Y.-C. Wang, T.-T. Wu, Y.-L. Chueh, A critical review on flexible Cu(In, Ga)Se₂ (CIGS) solar cells, Mater. Chem. Phys. 234 (2019) 329–344, <https://doi.org/10.1016/j.matchemphys.2019.04.066>.
- [10] N. Mufti, T. Amrillah, A. Taufiq, Aripriharta Sunaryono, M. Diantoro, Zulhadjri, H. Nur, Review of CIGS-based solar cells manufacturing by structural engineering,

- Sol. Energy 207 (2020) 1146–1157, <https://doi.org/10.1016/j.solener.2020.07.065>.
- [11] S.A. Khalate, R.S. Kate, R.J. Deokate, A review on energy economics and the recent research and development in energy and the Cu₂ZnSnS₄ (CZTS) solar cells: a focus towards efficiency, Sol. Energy 169 (2018) 616–633, <https://doi.org/10.1016/j.solener.2018.05.036>.
- [12] M. Ravindiran, C. Praveenkumar, Status review and the future prospects of CZTS based solar cell – a novel approach on the device structure and material modeling for CZTS based photovoltaic device, Renew. Sustain. Energy Rev. 94 (2018) 317–329, <https://doi.org/10.1016/j.rser.2018.06.008>.
- [13] M.L. Petrus, J. Schlipf, C. Li, T.P. Gujar, N. Giesbrecht, P. Müller-Buschbaum, M. Thelakkat, T. Bein, S. Hüttner, P. Docampo, Capturing the sun: a review of the challenges and perspectives of perovskite solar cells, Advanced Energy Materials 7 (2017) 1700264, <https://doi.org/10.1002/aenm.201700264>.
- [14] M.I.H. Ansari, A. Qurashi, M.K. Nazeeruddin, Frontiers, opportunities, and challenges in perovskite solar cells: a critical review, J. Photochem. Photobiol. C Photochem. Rev. 35 (2018) 1–24, <https://doi.org/10.1016/j.jphotochemrev.2017.11.002>.
- [15] S. Liu, Y. Guan, Y. Sheng, Y. Hu, Y. Rong, A. Mei, H. Han, A review on additives for halide perovskite solar cells, Advanced Energy Materials 10 (2019) 1902492, <https://doi.org/10.1002/aenm.201902492>.
- [16] J. Gong, K. Sumathy, Q. Qiao, Z. Zhou, Review on dye-sensitized solar cells (DSSCs): advanced techniques and research trends, Renew. Sustain. Energy Rev. 68 (2017) 234–246, <https://doi.org/10.1016/j.rser.2016.09.097>.
- [17] N. Roslan, M.E. Ya'acob, M.A.M. Radzi, Y. Hashimoto, D. Jamaludin, G. Chen, Dye Sensitized Solar Cell (DSSC) greenhouse shading: new insights for solar radiation manipulation, Renew. Sustain. Energy Rev. 92 (2018) 171–186, <https://doi.org/10.1016/j.rser.2018.04.095>.
- [18] D. Devadiga, M. Selvakumar, P. Shetty, M.S. Santosh, Dye-Sensitized solar cell for indoor applications: a mini-review, J. Electron. Mater. 50 (2021) 3187–3206, <https://doi.org/10.1007/s11664-021-08854-3>.
- [19] Z. Li, H.H. Tan, C. Jagadish, L. Fu, III–V semiconductor single nanowire solar cells: a review, Advanced Materials Technologies 3 (2018) 1800005, <https://doi.org/10.1002/admt.201800005>.
- [20] P. Colter, B. Hagar, S. Bedair, Tunnel junctions for III-V multijunction solar cells review, Crystals 8 (2018) 445, <https://doi.org/10.3390/crys8120445>.
- [21] V. Raj, H.H. Tan, C. Jagadish, Non-epitaxial carrier selective contacts for III-V solar cells: a review, Applied Materials Today 18 (2020) 100503, <https://doi.org/10.1016/j.apmt.2019.100503>.
- [22] J. Li, A. Aierken, Y. Liu, Y. Zhuang, X. Yang, J.H. Mo, R.K. Fan, Q.Y. Chen, S. Y. Zhang, Y.M. Huang, Q. Zhang, A brief review of high efficiency III-V solar cells for space application, Frontiers of Physics 8 (2021) 657, <https://doi.org/10.3389/fphy.2020.631925>.
- [23] M. Carmodya, S. Mallick, J. Margetis, R. Kodama, T. Biegala, D. Xu, P. Bechmann, J.W. Garland, S. Sivananthan, Single-crystal II–VI on Si single-junction and tandem solar cells, Appl. Phys. Lett. 96 (2010) 153502, <https://doi.org/10.1063/1.3386529>.
- [24] J.W. Garland, T. Biegala, M. Carmody, C. Gilmore, S. Sivananthan, Next-generation multijunction solar cells: the promise of II–VI materials, J. Appl. Phys. 109 (2011) 102423, <https://doi.org/10.1063/1.3582902>.
- [25] I.R. Chávez Urbiola, J.A. Bernal Martínez, J. Hernández Borja, C.E. Pérez García, R. Ramírez Bon, Y.V. Vorobiev, Combined CBD-CVD technique for preparation of II–VI semiconductor films for solar cells, Energy Procedia 57 (2014) 24–31, <https://doi.org/10.1016/j.egypro.2014.10.004>.
- [26] X. Zhang, D. Wu, H. Geng, Heterojunctions based on II–VI compound semiconductor one-dimensional nanostructures and their optoelectronic applications, Crystals 7 (2017) 307, <https://doi.org/10.3390/crys7100307>.
- [27] R. Kisslinger, W. Hua, K. Shankar, Bulk heterojunction solar cells based on blends of conjugated polymers with II–VI and IV–VI inorganic semiconductor quantum dots, Polymers 9 (2017) 35, <https://doi.org/10.3390/polym9020035>.
- [28] J.H. Song, S. Jeong, Colloidal quantum dot based solar cells: from materials to devices, Nano Convergence 4 (2017) 21, <https://doi.org/10.1186/s40580-017-0115-0>.
- [29] H. Choi, S. Jeong, A review on eco-friendly quantum dot solar cells: materials and manufacturing processes, International Journal of Precision Engineering and Manufacturing-Green Technology 5 (2018) 349–358, <https://doi.org/10.1007/s40684-018-0037-2>.
- [30] S. Birdoğan, M. Karabulut, Comparison of the effects of different ionic liquid-gels on the efficiencies of the PbSe, PbS and PbTe quantum dot sensitized solar cells, Opt. Mater. 111 (2021) 110603, <https://doi.org/10.1016/j.optmat.2020.110603>.
- [31] W. Shockley, The theory of p-n junctions in semiconductors and p-n junction transistors, The Bell System Technical Journal 28 (1949) 435–489, <https://doi.org/10.1002/j.1538-7305.1949.tb03645.x>.
- [32] M.A. Green, K. Emery, Y. Hishikawa, W. Warta, E.D. Dunlop, Solar cell efficiency tables (version 39), Progress in Photovoltaics 20 (2012) 12–20, <https://doi.org/10.1002/pip.2163>.
- [33] M.A. Green, K. Emery, Y. Hishikawa, W. Warta, E.D. Dunlop, Solar cell efficiency tables (version 40), Progress in Photovoltaics 20 (2012) 606–614, <https://doi.org/10.1002/pip.2267>.
- [34] M.A. Green, K. Emery, Y. Hishikawa, W. Warta, E.D. Dunlop, Solar cell efficiency tables (version 41), Progress in Photovoltaics 21 (2013) 1–11, <https://doi.org/10.1002/pip.2352>.
- [35] M.A. Green, K. Emery, Y. Hishikawa, W. Warta, E.D. Dunlop, Solar cell efficiency tables (version 42), Progress in Photovoltaics 21 (2013) 827–837, <https://doi.org/10.1002/pip.2404>.
- [36] M.A. Green, K. Emery, Y. Hishikawa, W. Warta, E.D. Dunlop, Solar cell efficiency tables (version 43), Progress in Photovoltaics 23 (2015) 1–9, <https://doi.org/10.1002/pip.2573>.
- [37] M.A. Green, K. Emery, Y. Hishikawa, W. Warta, E.D. Dunlop, Solar cell efficiency tables (version 46), Progress in Photovoltaics 23 (2015) 805–812, <https://doi.org/10.1002/pip.2637>.
- [38] M.A. Green, K. Emery, Y. Hishikawa, W. Warta, E.D. Dunlop, Solar cell efficiency tables (version 47), Progress in Photovoltaics 24 (2016) 3–11, <https://doi.org/10.1002/pip.2728>.
- [39] M.A. Green, K. Emery, Y. Hishikawa, W. Warta, E.D. Dunlop, Solar cell efficiency tables (version 48), Progress in Photovoltaics 24 (2016) 905–913, <https://doi.org/10.1002/pip.2788>.
- [40] M.A. Green, K. Emery, Y. Hishikawa, W. Warta, E.D. Dunlop, Solar cell efficiency tables (version 49), Progress in Photovoltaics 25 (2017) 3–13, <https://doi.org/10.1002/pip.2855>.
- [41] M.A. Green, K. Emery, Y. Hishikawa, W. Warta, E.D. Dunlop, Solar cell efficiency tables (version 50), Progress in Photovoltaics 25 (2017) 668–676, <https://doi.org/10.1002/pip.2909>.
- [42] M.A. Green, K. Emery, Y. Hishikawa, W. Warta, E.D. Dunlop, Solar cell efficiency tables (version 52), Progress in Photovoltaics 26 (2018) 427–436, <https://doi.org/10.1002/pip.3040>.
- [43] M.A. Green, K. Emery, Y. Hishikawa, W. Warta, E.D. Dunlop, Solar cell efficiency tables (version 54), Progress in Photovoltaics 27 (2019) 565–575, <https://doi.org/10.1002/pip.3171>.
- [44] M.A. Green, K. Emery, Y. Hishikawa, W. Warta, E.D. Dunlop, Solar cell efficiency tables (version 55), Progress in Photovoltaics 28 (2020) 3–15, <https://doi.org/10.1002/pip.3228>.
- [45] M.A. Green, Accurate expressions for solar cell fill factors including series and shunt resistances, Appl. Phys. Lett. 108 (2016) 081111, <https://doi.org/10.1063/1.4942660>.
- [46] R.M. Corless, G.H. Gonnet, D.E.G. Hare, D.J. Jeffrey, D.E. Knuth, On the Lambert W function, Adv. Comput. Math. 5 (1996) 329–359, <https://doi.org/10.1007/BF02124750>.
- [47] M. Abramowitz, I.A. Stegun, Handbook of Mathematical Functions with Formulas, Graphs, and Mathematical Tables, Dover Publications, New York, 1972, p. 14.
- [48] T.Y. Chow, What is a closed-form number? Am. Math. Mon. 106 (1999) 440–448, <https://doi.org/10.1080/000299890.1999.12005066>.
- [49] G. Arfken, Mathematical Methods for Physicists, Academic Press, Orlando, FL, 1985, pp. 282–283.
- [50] A. Schenck, U. Krumbein, Coupled defect-level recombination: theory and application to anomalous diode characteristics, J. Appl. Phys. 78 (1995) 3185–3192, <https://doi.org/10.1063/1.360007>.
- [51] H.J. Snaith, How should you measure your excitonic solar cells? Energy Environ. Sci. 5 (2012) 6513–6520, <https://doi.org/10.1039/c2ee03429>.
- [52] M.A. Green, Solar cell fill factors: general graph and empirical expressions, Solid State Electron. 24 (1981) 788–789, [https://doi.org/10.1016/0038-1101\(81\)90062-9](https://doi.org/10.1016/0038-1101(81)90062-9).
- [53] M.A. Green, Accuracy of analytical expressions for solar cell fill factors, Sol. Cell. 7 (1982) 337–340, [https://doi.org/10.1016/0379-6787\(82\)90057-6](https://doi.org/10.1016/0379-6787(82)90057-6).